

Recurrent mutations of the STAT6 DNA binding domain in primary mediastinal B-cell lymphoma

Olga Ritz,¹ Chrystelle Guiter,^{2,3} Flavia Castellano,^{2,3} Karola Dorsch,¹ Julia Melzner,¹ Jean-Philippe Jais,^{4,5} Gwendoline Dubois,^{2,6} Philippe Gaulard,^{2,3,6} Peter Möller,¹ and Karen Leroy^{2,3,6}

¹Abteilung für Pathologie des Universitätsklinikums Ulm, Ulm, Germany; ²Inserm, Unité U955, Créteil, France; ³Université Paris 12, Faculté de Médecine, Créteil, France; ⁴Assistance Publique—Hôpitaux de Paris (AP-HP), Hôpital Necker, Service de Biostatistiques, Paris, France; ⁵Université Paris Descartes, Paris, France; and ⁶AP-HP, Groupe Hospitalier Henri-Mondor Albert-Chenevier, Département de Pathologie, Créteil, France

Primary mediastinal B-cell lymphoma (PMBL) is a separate entity of aggressive B-cell lymphoma, characterized by a constitutive activation of janus kinase-signal transducer and activator of transcription (JAK-STAT) signaling pathway, also observed in Hodgkin lymphoma. Although many cancers exhibit constitutive JAK-STAT pathway activation, mutations of STAT genes have not been reported in neoplasms. Here, we show that MedB-1 PMBL-derived and L1236 Hodgkin-

derived cell lines and 20 of 55 (36%) PMBL cases harbor heterozygous missense mutations in STAT6 DNA binding domain, whereas no mutation was found in 25 diffuse large B-cell lymphoma samples. In 3 cases, somatic origin was indicated by the absence of the mutations in the nontumoral tissue. The pattern of STAT6 mutations was different from the classical features of somatic hypermutations. The mutant STAT6 proteins showed a decreased DNA binding ability in trans-

ected HEK cells, but no decrease in expression of STAT6 canonical target genes was observed in PMBL cases with a mutated STAT6 gene. Although the oncogenic properties of STAT6 mutant proteins remain to be determined, their recurrent selection in PMBL strongly argues for their involvement in the pathogenesis of this aggressive B-cell lymphoma. (Blood. 2009;114:1236-1242)

Introduction

Primary mediastinal B-cell lymphoma (PMBL) is recognized as a separate entity of aggressive B-cell lymphoma, with unique clinical, histologic, and biologic features.¹ This lymphoma presents as a mediastinal mass consisting of large B cells, that usually express little if any surface or cytoplasmic immunoglobulin and major histocompatibility complex class I and/or class II molecules and presumably derive from a subset of thymic B cells.² PMBL displays a constitutive activation of the janus kinase-signal transducer and activator of transcription (JAK-STAT) signaling pathway as indicated by the presence of nuclear phosphorylated (P) STAT6,³ which is also observed in Hodgkin lymphoma.^{4,5} STAT6 expression was shown to regulate cell proliferation and survival in a PMBL-derived cell line, MedB-1.⁶ These lymphomas harbor chromosomal gains of the *JAK2* gene⁷ and inactivating mutations of the suppressor of cytokine signaling (*SOCS1*) gene,⁸ which are also commonly found in Hodgkin lymphoma.^{9,10} Although *SOCS1* inactivation prevents STAT6 down-regulation and thereby contributes to STAT6 activity,⁶ the primary mechanism responsible for STAT6 activation remains unclear. PMBL do not secrete the specific cytokines (ie, interleukin [IL]-4 or IL-13) classically involved in the activation of this factor, unlike classical Hodgkin lymphoma,^{11,12} and *JAK2* inhibition only partially prevented STAT6 activation in MedB-1.³

The analysis of STAT6 functional properties by directed mutagenesis has shown that a mutation in the SH2 domain (STAT6 V547A/T548A) leads to the constitutive activation of STAT6.¹³ This mutation changes the conformation of the protein and

increases the stability of the monomeric and dimeric proteins, allowing STAT6VT mutant protein to undergo tyrosine phosphorylation, followed by DNA binding, in the absence of IL-4 stimulation. Transgenic mice expressing STAT6VT under control of the CD2 locus control region, which essentially directs expression to the T-cell compartment, show increased peripheral B-cell and decreased T-cell numbers¹⁴ and develop, in a small proportion of cases, a spontaneous lymphoproliferative disease of T-cell or B-cell mixed phenotype.¹⁵ These data prompted us to analyze the sequence of *STAT6* mRNA in MedB-1 and Karpas1106 PMBL-derived cell lines and in a series of 55 primary tumor samples. We found heterozygous mutations targeting the DNA binding domain in one cell line and 36% of the samples, and therefore, analyzed the histologic, clinical, and molecular characteristics of the PMBL cases with a *STAT6* mutation, as well as the functional properties of the mutant STAT6 proteins.

Methods

Tissue samples selection and DNA or RNA extraction

This study was approved by the Ethic Committee of the University of Ulm, Germany, and the Institutional Review Board "Comité de Protection des Personnes Ile de France IX," Créteil, France. A series of 55 PMBL and 25 diffuse large B-cell lymphoma cases (DLBCL) were retrieved from the files of the Institute of Pathology, Ulm, Germany, and of the Department of Pathology, Hospital Henri Mondor, Créteil, France. These lymphomas

Submitted March 9, 2009; accepted April 29, 2009. Prepublished online as *Blood* First Edition paper, May 7, 2009; DOI 10.1182/blood-2009-03-209759.

An Inside *Blood* analysis of this article appears at the front of this issue.

The online version of this article contains a data supplement.

The publication costs of this article were defrayed in part by page charge payment. Therefore, and solely to indicate this fact, this article is hereby marked "advertisement" in accordance with 18 USC section 1734.

© 2009 by The American Society of Hematology

samples, initially diagnosed between 1984 and 2007, showed the histologic features characteristic of these lymphoma types according to the recently updated World Health Organization (WHO) classification.¹ The PMBL samples had been previously immunophenotyped extensively and were included in several publications that contributed to define PMBL characteristic features.^{3,8,16-19} Tumor infiltration of the frozen samples was checked on hematoxylin eosin safran staining of tissue sections. Total RNA were extracted from frozen tissue samples with TRIzol reagent (Invitrogen) or RNeasy mini kit (QIAGEN) according to the manufacturer's instructions. Genomic DNA was extracted with proteinase K digestion, phenol chloroform phases separation, and ethanol precipitation.

Sequencing and quantitative polymerase chain reaction

Total RNA were reverse-transcribed with Superscript II (Invitrogen) and 500 ng poly(dT) or 300 ng random primers in a final volume of 20 μ L, according to the manufacturer's instructions, and diluted 1:5 or 1:10 for polymerase chain reaction (PCR). Genomic DNA and cDNA were amplified by PCR using primers and detailed protocol indicated in the supplemental methods (available on the *Blood* website; see the Supplemental Materials link at the top of the online article).

Purified PCR products were sequenced using BigDye Terminator version 3.1 Cycle sequencing kits (Applied Biosystems) and capillary electrophoresis (3130 Genetic analyzer; Applied Biosystems). Sequences were analyzed with Seqscape software (Applied Biosystems) and standard electropherogram reading programs (Chromas Lite, www.technelysium.com). Nucleotide changes detected on one strand were confirmed by sequencing the reverse strand. *STAT6* sequencing was performed on genomic DNA and cDNA in 25 cases (14 with and 11 without detected mutations), on cDNA only in 21 cases (4 with and 17 without detected mutations) or genomic DNA only in 9 cases (2 with and 7 without detected mutations), depending on the material available. The *SOCS1* alterations (mutations or microdeletions) were assessed on genomic DNA and cDNA (5 cases), on cDNA only (5 cases), or genomic DNA only (43 cases).

Genomic tumoral DNAs from the PMBL cases were also used for the quantitative analysis of the *JAK2* gene. Briefly, 50 ng DNA were amplified using the Bio-Rad Laboratories SYBR Green master mix and primers for *JAK2* and for *B2M* (supplemental Table 1) in a total reaction volume of 20 μ L in a Bio-Rad Laboratories I-cycler. Each PCR was run in quadruplicate, and the mean cycle threshold (Ct) values were used for further calculations. Relative *JAK2* gene dosage was calculated according to the $2^{-\Delta\Delta C_t}$ method.²⁰ Genomic DNA isolated from lymphocytes of 4 different healthy donors and from 7 frozen reactive tonsils were used to calculate the mean normal *JAK2* gene dosage. Tumor samples were considered to have a *JAK2* gain or amplification if the relative *JAK2* gene dosage was superior to mean normal plus 3 standard deviations.

Transfection, generation of the HEK stable transfectants, and reporter assays

Wild-type (WT) and double mutant (DM) *STAT6* expression vectors were obtained by PCR amplification of *STAT6* coding sequence using cDNA from Ramos and MedB-1 cell line, respectively, and primers containing *EcoRI* and *XhoI* restriction sites (in italics): *STAT6* forward: 5'-CGACGTGGAA177CTGTCTCTGTGGGGTCTG-3'; *STAT6* reverse: 5'-CAGTGCTCGAGCTCACCAACTGGGGTTGGCCCT-3'). PCR products were inserted into the multiple cloning site of pcDNA3.1 expression vector (Invitrogen) and verified by sequencing. Single mutants were obtained by directed mutagenesis of WT *STAT6* expression plasmids with the GeneEditor in Vitro Site-Directed Mutagenesis system (Promega). WT *STAT6* and DM *STAT6* expression plasmids or pcDNA-mock vector were transfected into HEK293 cell lines using Effectene Transfection Reagent (QIAGEN) according to the manufacturer's instructions. Twenty-four hours after transfection, 800 μ g/mL G418 (Invitrogen) were added to the medium, and HEK293 cells were cultured in the selection medium for 2 weeks before isolation of single clones or pooling transfected cells. During analysis, the transfected cells were maintained under 600 μ g/mL G418.

Firefly luciferase reporter vector containing (N3-luc) or not (control-luc) 3 copies of the N3-gamma-activated site (GAS) from *CSN2* (casein β) promoter (TTCtagGAA) were obtained from Panomic. The N4-luc vector, comprising 3 *STAT6* binding site from the *SOCS1* promoter (TTCcgag-GAA) upstream of the luciferase reporter gene was previously described.⁶ HEK293 cells were transiently cotransfected using effectene transfection reagent with control-luc, N3-luc, or N4-luc reporter constructs (1 μ g) in combination with either mock or WT *STAT6* or one of the mutated *STAT6* expression vectors (1 μ g). Forty nanograms of a *Renilla* luciferase reporter were added to each sample to normalize transfection efficiency. Luminescence intensity was measured using the luminometer Lumat FB12 (Berthold Technologies) and luciferase dual assay kit (Promega) according to the manufacturer's protocol.

Western blot analysis and immunohistochemistry

Western blot analyses were performed as previously described.⁶ Proteins were detected using antibodies against *STAT6* (M-200; sc-1698; Santa Cruz Biotechnology) 1:1000; P-*STAT6* (Tyr641; 9361; Cell Signaling) 1:1000; β -actin (clone AC-74; Sigma-Aldrich) 1:5000; HDAC1 (H-51; Santa Cruz Biotechnology) 1:1000.

Immunohistochemistry was performed on paraffin section of formalin-fixed tissue or on frozen sections. Paraffin sections were pretreated for 20 minutes by steamer boiling in Tris ethylenediaminetetraacetic acid (EDTA) buffer, pH 6.0. For detection of bound P-*STAT6* antibody, the EnVision detection system (Dako) was used with diaminobenzidine as substrate.²¹ The detection of P-*STAT6* protein was checked in control cells (ie, interstitial fibroblastoid cells and a subset of endothelial cells) present in each tissue sample. Samples without positive control cells were disregarded. P-*STAT6* staining of neoplastic cells was considered positive whenever more than 5% of neoplastic cells had nuclear staining.

Electrophoretic mobility shift assay

N4-GAS probe from *SOCS1* promoter (5'-AGGTCGACTTCCCAAGAACA-GAG-3' annealed with 5'-AGGCTCTGTTCTTGGGAAGTCGA-3') and N3-GAS probe from the *CSN2* (casein β) promoter (5'-AGGAGATTTCTAG-GAATTCATCC-3' annealed with 5'-AGGGGATTGAAATTCCTA-GAAATCT-3') were prepared. One microgram nuclear protein extracts from HEK293 stable pools (mock, WT *STAT6*, and DM *STAT6*) was incubated with ³²P-labeled N4- or N3-GAS probes, with or without 1 μ L anti-*STAT6* antibody (S-20; sc-621; Santa Cruz Biotechnology) or a 100-fold molar excess cold probe and were separated on a 4% native acrylamide gel.

Results

Recurrent mutations of *STAT6* DNA binding domain in MedB-1 cell line and PMBL primary tumors

We analyzed the entire coding sequence of *STAT6* mRNA in MedB-1 and Karpas1106 PMBL-derived cell lines. Direct sequencing of PCR products showed that Karpas1106 cells carried WT *STAT6* mRNA sequences, whereas MedB-1 cells exhibited 2 heterozygous missense mutations located in exon 12 (N417Y and N430T), which encodes part of the DNA binding domain. We amplified MedB-1 exon 12 genomic DNA and sequenced cloned PCR products. Seven clones showed both N417Y and N430T mutations, and 2 were WT, indicating that both mutations were located on the same allele. These mutations were detected in the parental tumor from which this cell line was established,²² but were absent in fibroblasts isolated from the same patient.

To evaluate the relevance of these mutations in PMBL, we sequenced the region of the *STAT6* gene encoding amino acids L406 to R527 in 55 PMBL and 25 aggressive B-cell lymphomas of the diffuse large B-cell type. The DNA binding domain of *STAT6*

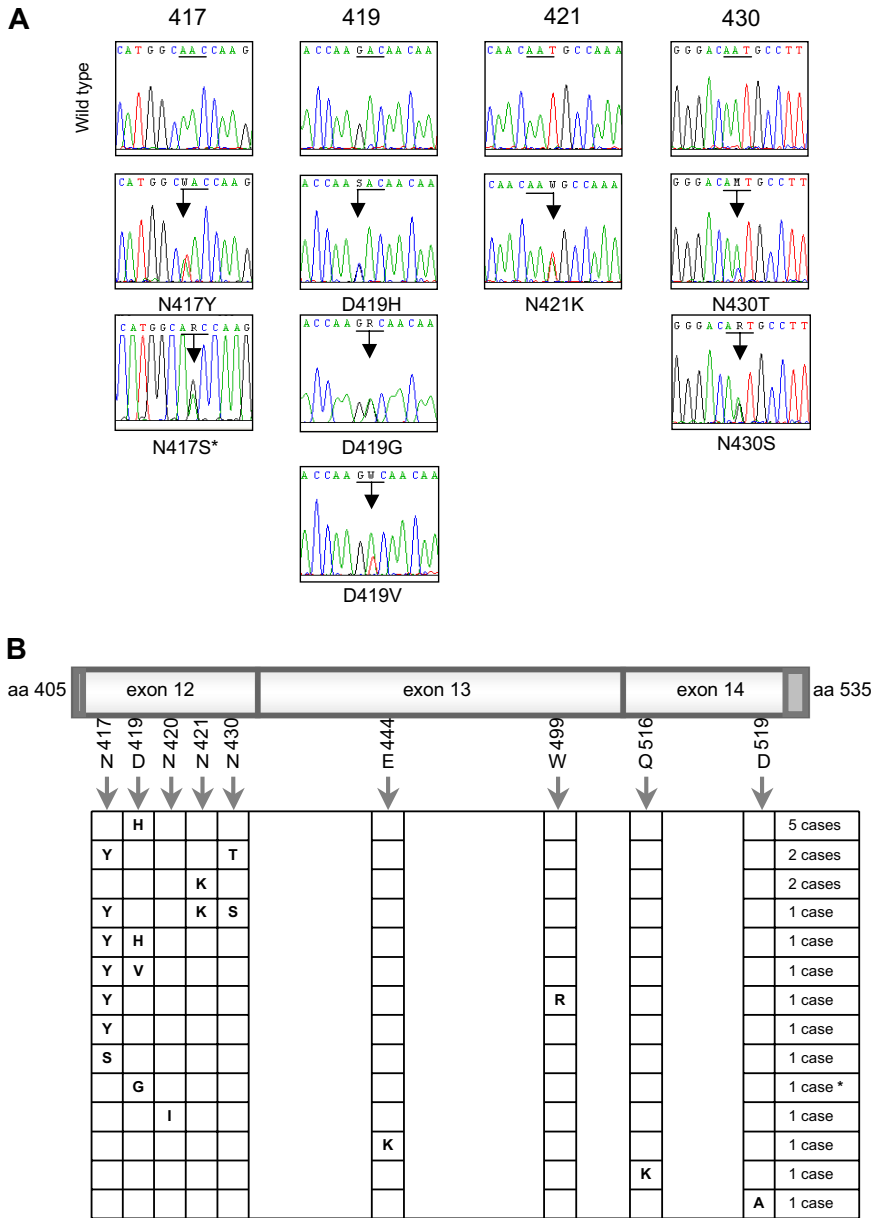


Figure 1. Heterozygous mutations in the DNA binding domain of STAT6 in PMBL. (A) Electropherograms showing partial *STAT6* cDNA sequences for the 4 most frequently mutated codons (underlined). Mixed nucleotides are lettered according to International Union of Pure and Applied Chemistry (IUPAC) international code. *This sequence was performed by PCR amplification of genomic DNA (no RNA available). (B) Schematic localization of mutations in the region spanning nucleotides 1216 to 1581, corresponding to exon 12 (minus 4 bases in the 5' dark gray part), exon 13, and exon 14 (minus 26 bases in the 3' dark gray part) of *STAT6* in the 20 mutated PMBL cases. *This case presents both a missense mutation of codon 419 and a silent mutation of codon 423 (c.A1269G, according to NM_003153.3).

was found to be mutated in 20 of 55 (36%) PMBL cases, whereas no mutation was detected in the 25 diffuse large B-cell lymphomas (Fisher exact test, $P < .001$). Interestingly, 6 PMBL cases had several missense mutations, and one case had both a missense and a silent mutation (Figure 1A). The 28 mutations that we detected were heterozygous and targeted preferentially A:T base pairs (20/28, exact binomial test, $P = .004$) and AA, AG, AT, or GA dinucleotides (Table 1). These mutations mostly affected exon 12, with 4 hotspots targeting amino acid 417, 419, 421, and 430, respectively (Figure 1B). Of note, D419 is the site of a known polymorphism (D419N), which was not observed in the 80 lymphoma samples analyzed. Sequencing of genomic DNA derived from nontumoral tissue of 2 mutated PMBL cases revealed WT sequence, supporting a somatic origin of the mutations, as observed in MedB-1/PMBL parental tumor.

As Hodgkin lymphoma cell lines also exhibit *STAT6* activation⁵ and share some features with PMBL in gene expression profiles,^{19,23} we sequenced the same region of *STAT6* mRNA in 4 classical Hodgkin-derived cell lines. Strikingly, L1236 cell line,

previously reported to have *STAT6* gene amplification and overexpression²⁴ showed only expression of a mutated *STAT6* allele, encoding N417Y hotspot mutation and D419N polymorphic change (Figure S1), while no mutation was detected in L428, L540, and KMH2 mRNA sequences.

Characteristics of the PMBL cases with a mutation of *STAT6* gene

The 20 PMBL cases with a mutated *STAT6* gene exhibited similar histologic features (clear cells and fibrosis) and clinical characteristics as the 35 nonmutated ones (Table 2). Twelve PMBL cases previously shown to have a PMBL molecular signature¹⁹ had mutations in *STAT6* gene (7 cases) or not (5 cases). Intriguingly, the 7 cases with multiple *STAT6* nucleotide changes presented a male predominance (M/F ratio = 5/2) and a younger age at diagnosis (median, 32 years) compared with the 13 cases with single nucleotide changes (M/F ratio = 2/11, $P = .02$, Fisher exact test; median age at diagnosis 41 years, $P = .07$, Wilcoxon rank sum

Table 1. Mutation characteristics in STAT6 exons 12-14

	No. of mutations observed	No. of motifs or dinucleotides in sequence	No. of expected mutations*	Observed/expected mutations ratio	P†
Transversions/transitions					
All	22/6		18.7/9.3	1.83	.230
A:T base pairs	20	158	12.1	1.65	.004
G:C base pairs	8	207	15.9	0.5	
Dinucleotides					
AA‡	13	20	3.077	4.225	< .001
AC	4	19	2.923	1.368	.520
AG‡	7	20	3.077	2.275	.025
AT‡	7	13	2.000	3.500	.001
CA	8	27	4.154	1.926	.056
CC	0	34	5.231	0.000	.007
CG	0	9	1.385	0.000	.372
CT	1	32	4.923	0.203	.051
GA‡	10	23	3.538	2.826	.001
GC	1	24	3.692	0.271	.161
GG	0	33	5.077	0.000	.007
GT	0	24	3.692	0.000	.041
TA	0	2	0.308	0.000	> .999
TC	0	26	4.000	0.000	.025
TG	5	42	6.462	0.774	.671
TT	0	16	2.462	0.000	.155

*Expected mutation frequencies were calculated according to the sequence composition, assuming random targeting of the mutations at a 28/365 rate for single nucleotide changes and 56/364 rate for dinucleotide mutations.

†Statistical comparisons were done with the exact binomial test, which compares the observed frequency to the expected one under null hypothesis.

‡Dinucleotides significantly targeted by mutations.

test), suggesting that a highly mutated phenotype might delineate a particular subset of PMBL patients.

P-STAT6 nuclear staining was detected in the nuclei of tumor cells in 31 of 35 (88%) cases that could be evaluated (Table 2). It was present in all STAT6 mutated cases, but also in a large fraction of nonmutated cases, indicating that activation of STAT6 can occur in the absence of mutation of the gene. SOCS1 gene deletions and/or mutations were observed in 34 of 52 (65%) PMBL cases. JAK2 gain or amplification was observed in 22 of 47 (47%) PMBL

cases, at a similar frequency as that recently reported in a high resolution CGH array study.²⁵ SOCS1 gene alterations and JAK2 amplifications were present both in STAT6 mutated cases and nonmutated cases (Table 2). Of the 47 cases that could be analyzed for all 3 genes, 5 showed no genetic alteration, 20 showed one alteration, 17 showed 2 alterations, and 5 cases had alterations of the 3 genes. Thus, it appears that the different genetic alterations of the JAK-STAT signaling pathway are not mutually exclusive in PMBL, suggesting additive effects.

Table 2. Characteristics of the cases according to the presence or absence of a STAT6 mutation detected in exons 12-14

	STAT6 mutation (n = 20)	No STAT6 mutation (n = 35)	P*
Median age at diagnosis, y (range)	37.5 (22-59)	32 (17-73)	.43
Females/males	13/7	15/20	.16
Ann Arbor stage at diagnosis			
I-II	11	16	.71
III-IV	3	7	
Unknown	6	12	
P-STAT6 staining			
Positive	14	17	.13
Negative	0	4	
Not evaluable	6	14	
SOCS1 gene alteration			
Present	15	19	.14
Absent	4	14	
Not determined	1	2	
JAK2 gene amplification			
Present	7	15	.76
Absent	10	15	
Not determined	3	5	

*Age at diagnosis was compared with Wilcoxon rank test and the other characteristics were compared with Fisher exact test (using only informative cases).

Functional properties of STAT6 mutant proteins

To evaluate the functional properties of the mutated STAT6 proteins, we transfected the HEK293 STAT6 deficient cell line with expression vectors encoding either WT or N417/N430 DM STAT6, expressed in MedB-1/parental tumor and case 52. Independent stable pools and clones exhibited the same levels of basal- and IL-4-induced STAT6 phosphorylation (Figure 2A). DM STAT6 transfectants showed a decreased DNA binding activity on both N4- and N3-GAS sites (TTC[N] × GAA), compared with WT STAT6 expressing cells, although similar amounts of STAT6 and P-STAT6 were detected in the nucleus of WT and DM STAT6 expressing cells (Figure 2B). We hypothesized that the diminished DNA binding activity of STAT6 mutants might affect their ability to activate the expression of N4- or N3-GAS driven reporters. As shown in Figure 2C, HEK293 cells transiently transfected with DM or with N417Y, D419H, N421K, N430T STAT6 single mutants displayed reduced N4- and N3-sites driven reporter expression, compared with WT STAT6 expressing cells, although achieving similar levels of P-STAT6 after IL-4 stimulation.

The decreased ability of STAT6 mutants to activate transcription was surprising considering the strong STAT6 signature previously reported in gene expression profiling studies of PMBL.^{19,23} We therefore compared the levels of expression of several genes

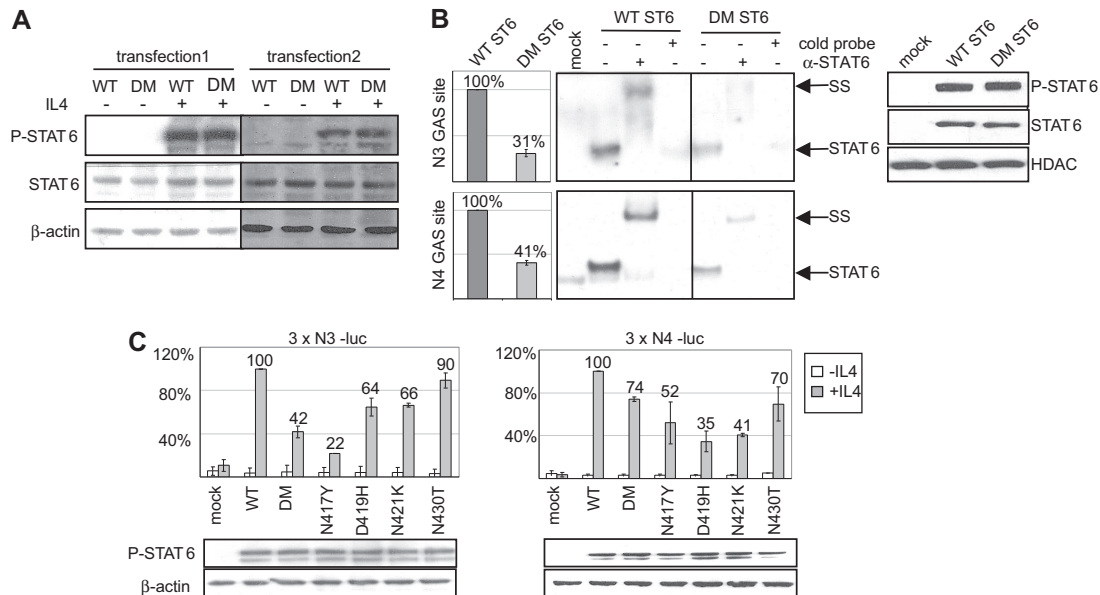


Figure 2. Functional properties of mutated STAT6 proteins in HEK293 transfectant cells. (A) Transfected HEK293 cells expressing WT or N417/N430 DM STAT6, selected with G418 (transfection 1, pools; 2, single clones), were incubated (+) or not (–) with 10 ng/mL IL-4 for 24 hours. Western blot analyses of total protein extracts (7 μ g) probed with antibodies against P-STAT6 (Tyr-641), total STAT6, and β -actin are shown. (B) EMSA was prepared using 1 μ g nuclear extracts from mock transfected cells, WT or DM STAT6 HEK293 pools, stimulated with 10 ng/mL IL-4 for 6 hours, and radiolabeled N3-GAS or N4-GAS probes. Incubation was performed with (+) or without (–) an antibody against STAT6 or an excess of cold probe. The protein/DNA complexes were electrophoresed on the same gel and are assembled side by side in the figure for better comparison. The position of the STAT6 containing complexes and of the complexes supershifted (SS) by the antibody are indicated. Phosphorimager quantification of the radiolabeled complexes is shown in the left plots, and Western blot analysis of P-STAT6 and HDAC, used as a loading control, in nuclear extracts is shown in the right plot. (C) HEK293 cells were cotransfected with expression vectors for WT STAT6, single or DM STAT6 mutants, or a control mock-vector, together with 3 \times N3-luc (left plot) or with 3 \times N4-luc (right plot) luciferase reporter constructs. The diagrams show the mean percentage of luciferase activity, after normalization for transfection efficacy, in cells treated (■) or not (□) with 10 ng/mL IL-4 for 20 hours, compared with WT STAT6 expressing cells (set to 100%). Error bars show the SD (3 independent experiments). The amount of P-STAT6 in total protein extracts of IL-4-treated cells, detected by immunoblotting, is shown in the bottom panel.

that contain confirmed STAT6 binding motifs²⁶ in the 5 nonmutated and the 7 mutated cases that had been analyzed with microarrays as part of a larger study.¹⁹ The levels of expression of these genes were similar in the 2 groups (Table 3), indicating that these mutations did not significantly impair the expression of these endogenous STAT6 targets in lymphoma cells.

Discussion

PMBL is characterized by a constitutive activation of the JAK-STAT pathway, associated with *SOCS1* gene defects and/or *JAK2* gene amplification, leading to STAT6 phosphorylation and DNA

binding activity. In this study, we identified mutations affecting the STAT6 DNA binding domains in 20 of 55 (36%) PMBL cases, but none of the 25 DLBCL tested. Although the constitutive activation of STAT proteins is a common finding in hematopoietic and nonhematopoietic cancers,²⁷ this is the first observation of recurrent *STAT6* gene mutations associated with human cancer. The 7 PMBL cases with several nucleotide changes in *STAT6* sequence were mostly young males, and 3 of them had a rapidly fatal disease, highlighting the need of larger studies to address the association of *STAT6* mutation with clinical presentation and outcome. It is noteworthy that the L1236 classical Hodgkin lymphoma cell line, which harbors an amplification of the *STAT6* gene²⁴ and which depends on IL-13 signaling for cell proliferation and viability,²⁸

Table 3. Expression of loci containing one or more confirmed STAT6 binding motifs in PMBL cases

Gene	Microarray ID	No <i>STAT6</i> mutation (n = 5)*	<i>STAT6</i> mutation (n = 7)*	Fold change†	P‡
<i>FCER2</i>	35220	–1.26	–0.24	2.02	.26
<i>FCER2</i>	17521	–1.37	–0.36	2.01	.37
<i>IL4</i>	25233	–0.37	0.03	1.32	.32
<i>IL4</i>	34968	–0.46	–0.08	1.30	.40
<i>IL4R</i>	28597	1.05	1.41	1.28	.15
<i>IL4R</i>	19256	1.69	2.09	1.32	.25
<i>CCL17</i>	29233	–1.26	–0.82	1.36	.60
<i>CD40</i>	27399	0.11	0.53	1.34	.07
<i>CD40</i>	16913	0.10	0.45	1.28	.12
<i>BCL2L1</i>	16454	0.02	–0.15	0.89	.30
<i>BCL2L1</i>	24267	0.10	–0.03	0.92	.53
<i>IL4I1</i>	149016	2.25	2.40	1.11	.75
<i>IL4I1</i>	149017	1.57	1.94	1.29	.23

*Mean expression levels (log₂) in cases with (n = 7) or without (n = 5) *STAT6* mutation from Rosenwald et al.¹⁹

†Fold change, ratio of mean expression in mutated cases relative to WT cases.

‡P values (by Student *t* test) were not corrected for multiple comparisons.

had an identical hotspot mutation in STAT6 DNA binding domain. This finding extends the list of genetic alterations common to PMBL and classical Hodgkin lymphoma, such as *REL* and *JAK2* genes gain/amplification⁹ and *SOCS1* gene deletions/mutations,¹⁰ and supports the concept of a continuum between these 2 diseases, as acknowledged by the recognition of intermediate “gray zone” lymphomas in the 2008 updated WHO classification.¹

Mutations of oncogenes have been shown to occur through aberrant somatic hypermutation (SHM) in DLBCL and PMBL.²⁹ The mutations observed in *STAT6* gene were strikingly different of the classical features of SHM.³⁰ These mutations were mostly transversions, whereas SHM is characterized by transitions occurring twice as frequently as transversions; they mostly targeted A:T base pairs, whereas SHM affects mostly G:C base pairs; they were located 8.5 kb from the transcriptional start site, whereas SHM mutations are usually located 2 kb from the start site. It is interesting to note that hypermutation of *BCL6* regulatory region was previously reported to differ in PMBL and DLBCL.³¹ The pattern of somatic mutations reflects both their mechanism of origin and their selection during tumor growth. Because *STAT6* mutations affect the coding sequence, the pattern of mutation may be biased by the selection process. Nevertheless, these results suggest that some atypical SHM or other mutational mechanisms may occur in PMBL.

In the last years, hypomorphic mutations of the *STAT3* gene, most frequently located in the DNA binding domain, have been reported to be responsible for autosomal dominant and sporadic hyper-immunoglobulin E (IgE) syndrome, a primary immunodeficiency defect,³² and mutations of the *STAT1* gene have been associated with type I interferon immunodeficiency.³³ These mutations were shown to be associated with impaired DNA binding ability. In line with these observations, the analysis of the functional properties of *STAT6* mutants identified in PMBL, also revealed an impaired function in HEK293 cells in electrophoretic mobility shift assay (EMSA) and reporter assays. Three (N417, D419, and N421) of the 4 hotspot mutations are located in a region that was identified as an important DNA recognition element in the crystal structure of *STAT1*³⁴ and *STAT3*³⁵ dimers bound to DNA, and this may account for their diminished ability to activate *STAT6* synthetic reporter constructs. The fourth hot spot (N430), which had a weak effect in these assays and was never observed as sole mutation, corresponds to a residue that is absolutely conserved in human and mouse *STAT* proteins.

The arguments for the involvement of *STAT6* mutations in lymphomagenesis are (1) their frequency in PMBL, indicating an *in vivo* selection during transformation and/or progression; (2) the presence of mutational hotspots; (3) the fact that they target an activated signaling pathway; and (4) their presence in a Hodgkin cell line with concordant gene amplification. However, the mecha-

nisms through which these mutations affect tumor growth remain elusive. Although *STAT6* mutants showed an impaired function on short synthetic promoters in a heterologous cell system, PMBL samples did not show a decreased expression of classical *STAT6* targets. This apparent discrepancy may be because the highly complex *in vivo* transcriptional regulation coordinated by *STAT6* is not addressed in HEK cells transfections.

Altogether, our results show that the region encoding the DNA binding domain of *STAT6* is the target of recurrent mutations in PMBL but not DLBCL. Further investigations are required to identify the mutational mechanisms involved and the oncogenic function associated with these mutations. This observation opens a wide field of investigation to determine the spectrum and functional consequences of *STAT* mutations in tumors, which are critical points in regard to the current development of anti-JAK targeted therapies.

Acknowledgments

We thank M. Dyer for providing the Karpas1106 cell line, M.C. Baglin (Hospital Foch, Suresnes), B. Petit (CHU Limoges), M. Parrens (CHU Bordeaux), and J. Brière (Hospital Saint-Louis, Paris) for providing PMBL samples. We are grateful to M. Baia for her technical help, to I. Dusanter and O. Bernard for helpful discussions, and to P.H. Roméo for critically reading of the manuscript.

This study was supported by a grant of the Institut National du Cancer (INCa) and German Academic Exchange Service (DAAD). O.R. was supported by a grant of the Deutsche Forschungsgemeinschaft (DFG, RI 1915/1-1).

Authorship

Contribution: O.R. and C.G. contributed equally to this study; O.R., C.G., and F.C. designed and performed experiments, interpreted the results, and corrected the manuscript; K.D., J.M., and G.D. performed experiments; J.P.J. performed statistical analysis; P.M. and P.G. selected and reviewed the lymphoma cases and contributed to the manuscript; and K.L. designed and interpreted experiments and wrote the manuscript.

Conflict-of-interest disclosure: The authors declare no competing financial interests.

Correspondence: Peter Möller, Institut für Pathologie des Universitätsklinikums Ulm, Albert-Einstein-Allee 11, D-89081 Ulm, Germany; e-mail: peter.moeller@uniklinik-ulm.de; or Karen Leroy, Inserm, Unité 955, Département de Pathologie, Hôpital Henri Mondor, 51 avenue du maréchal de Lattre de Tassigny, Créteil, F-94000, France; e-mail: karen.leroy@hmn.aphp.fr.

References

- Swerdlow SH, Campo E, Harris NL. *WHO Classification of Tumors of Haematopoietic and Lymphoid Tissues*. 4th Ed. Lyon, France: International Agency for Research on Cancer; 2008.
- Barth TF, Leithauser F, Joos S, Bentz M, Moller P. Mediastinal (thymic) large B-cell lymphoma: where do we stand? *Lancet Oncol*. 2002;3:229-234.
- Guitier C, Dusanter-Fourt I, Copie-Bergman C, et al. Constitutive *STAT6* activation in primary mediastinal large B-cell lymphoma. *Blood*. 2004; 104:543-549.
- Mottok A, Renne C, Willenbrock K, Hansmann ML, Brauning A. Somatic hypermutation of *SOCS1* in lymphocyte-predominant Hodgkin lymphoma is accompanied by high *JAK2* expression and activation of *STAT6*. *Blood*. 2007;110:3387-3390.
- Skinnider BF, Elia AJ, Gascoyne RD, et al. Signal transducer and activator of transcription 6 is frequently activated in Hodgkin and Reed-Sternberg cells of Hodgkin lymphoma. *Blood*. 2002;99:618-626.
- Ritz O, Guitier C, Dorsch K, et al. *STAT6* activity is regulated by *SOCS-1* and modulates *BCL-XL* expression in primary mediastinal B-cell lymphoma. *Leukemia*. 2008;22:2106-2110.
- Bentz M, Barth TF, Bruderlein S, et al. Gain of chromosome arm 9p is characteristic of primary mediastinal B-cell lymphoma (MBL): comprehensive molecular cytogenetic analysis and presentation of a novel MBL cell line. *Genes Chromosomes Cancer*. 2001;30:393-401.
- Melzner I, Bucur AJ, Bruderlein S, et al. Biallelic mutation of *SOCS-1* impairs *JAK2* degradation and sustains phospho-*JAK2* action in the MedB-1 mediastinal lymphoma line. *Blood*. 2005;105: 2535-2542.
- Joos S, Granzow M, Holtgreve-Grez H, et al. Hodgkin's lymphoma cell lines are characterized

- by frequent aberrations on chromosomes 2p and 9p including REL and JAK2. *Int J Cancer*. 2003;103:489-495.
10. Weniger MA, Melzner I, Menz CK, et al. Mutations of the tumor suppressor gene SOCS-1 in classical Hodgkin lymphoma are frequent and associated with nuclear phospho-STAT5 accumulation. *Oncogene*. 2006;25:2679-2684.
 11. Kapp U, Yeh WC, Patterson B, et al. Interleukin 13 is secreted by and stimulates the growth of Hodgkin and Reed-Sternberg cells. *J Exp Med*. 1999;189:1939-1946.
 12. Skinnider BF, Elia AJ, Gascoyne RD, et al. Interleukin 13 and interleukin 13 receptor are frequently expressed by Hodgkin and Reed-Sternberg cells of Hodgkin lymphoma. *Blood*. 2001;97:250-255.
 13. Daniel C, Salvekar A, Schindler U. A gain-of-function mutation in STAT6. *J Biol Chem*. 2000;275:14255-14259.
 14. Bruns HA, Schindler U, Kaplan MH. Expression of a constitutively active Stat6 in vivo alters lymphocyte homeostasis with distinct effects in T and B cells. *J Immunol*. 2003;170:3478-3487.
 15. Kaplan MH, Sehra S, Chang HC, O'Malley JT, Mathur AN, Bruns HA. Constitutively active STAT6 predisposes toward a lymphoproliferative disorder. *Blood*. 2007;110:4367-4369.
 16. Copie-Bergman C, Boulland ML, Dehouille C, et al. Interleukin 4-induced gene 1 is activated in primary mediastinal large B-cell lymphoma. *Blood*. 2003;101:2756-2761.
 17. Joos S, Otano-Joos MI, Ziegler S, et al. Primary mediastinal (thymic) B-cell lymphoma is characterized by gains of chromosomal material including 9p and amplification of the REL gene. *Blood*. 1996;87:1571-1578.
 18. Paulli M, Strater J, Gianelli U, et al. Mediastinal B-cell lymphoma: a study of its histomorphologic spectrum based on 109 cases. *Hum Pathol*. 1999;30:178-187.
 19. Rosenwald A, Wright G, Leroy K, et al. Molecular diagnosis of primary mediastinal B cell lymphoma identifies a clinically favorable subgroup of diffuse large B cell lymphoma related to Hodgkin lymphoma. *J Exp Med*. 2003;198:851-862.
 20. Livak KJ, Schmittgen TD. Analysis of relative gene expression data using real-time quantitative PCR and the 2(-DeltaDelta C(T)) Method. *Methods*. 2001;25:402-408.
 21. Moldenhauer G, Popov SW, Wotschke B, et al. AID expression identifies interfollicular large B cells as putative precursors of mature B-cell malignancies. *Blood*. 2006;107:2470-2473.
 22. Moller P, Bruderlein S, Strater J, et al. MedB-1, a human tumor cell line derived from a primary mediastinal large B-cell lymphoma. *Int J Cancer*. 2001;92:348-353.
 23. Savage KJ, Monti S, Kutok JL, et al. The molecular signature of mediastinal large B-cell lymphoma differs from that of other diffuse large B-cell lymphomas and shares features with classical Hodgkin lymphoma. *Blood*. 2003;102:3871-3879.
 24. Feys T, Poppe B, De Preter K, et al. A detailed inventory of DNA copy number alterations in four commonly used Hodgkin's lymphoma cell lines. *Haematologica*. 2007;92:913-920.
 25. Lenz G, Wright GW, Emre NC, et al. Molecular subtypes of diffuse large B-cell lymphoma arise by distinct genetic pathways. *Proc Natl Acad Sci U S A*. 2008;105:13520-13525.
 26. Hebenstreit D, Wirmsberger G, Horejs-Hoeck J, Duschl A. Signaling mechanisms, interaction partners, and target genes of STAT6. *Cytokine Growth Factor Rev*. 2006;17:173-188.
 27. Constantinescu SN, Girardot M, Pecquet C. Mining for JAK-STAT mutations in cancer. *Trends Biochem Sci*. 2008;33:122-131.
 28. Trieu Y, Wen XY, Skinnider BF, et al. Soluble interleukin-13R α 2 decoy receptor inhibits Hodgkin's lymphoma growth in vitro and in vivo. *Cancer Res*. 2004;64:3271-3275.
 29. Rossi D, Cerri M, Capello D, et al. Aberrant somatic hypermutation in primary mediastinal large B-cell lymphoma. *Leukemia*. 2005;19:2363-2366.
 30. Odegard VH, Schatz DG. Targeting of somatic hypermutation. *Nat Rev Immunol*. 2006;6:573-583.
 31. Malpeli G, Barbi S, Moore PS, et al. Primary mediastinal B-cell lymphoma: hypermutation of the BCL6 gene targets motifs different from those in diffuse large B-cell and follicular lymphomas. *Haematologica*. 2004;89:1091-1099.
 32. Minegishi Y, Saito M, Tsuchiya S, et al. Dominant-negative mutations in the DNA-binding domain of STAT3 cause hyper-IgE syndrome. *Nature*. 2007;448:1058-1062.
 33. Chappier A, Boisson-Dupuis S, Jouanguy E, et al. Novel STAT1 alleles in otherwise healthy patients with mycobacterial disease. *PLoS Genet*. 2006;2:e131.
 34. Chen X, Vinkemeier U, Zhao Y, Jeruzalmi D, Darnell JE Jr, Kuriyan J. Crystal structure of a tyrosine phosphorylated STAT-1 dimer bound to DNA. *Cell*. 1998;93:827-839.
 35. Becker S, Groner B, Muller CW. Three-dimensional structure of the Stat3 β homodimer bound to DNA. *Nature*. 1998;394:145-151.